Water Research 172 (2020) 115474

Contents lists available at ScienceDirect

Water Research

journal homepage: www.elsevier.com/locate/watres

Evaluation of the integration of P recovery, polyhydroxyalkanoate production and short cut nitrogen removal in a mainstream wastewater treatment process

Oriol Larriba, Eric Rovira-Cal, Zivko Juznic-Zonta, Albert Guisasola*, Juan Antonio Baeza

GENOCOV. Departament d'Enginyeria Química, Biològica i Ambiental. Escola d'Enginyeria. Universitat Autònoma de Barcelona, 08193, Bellaterra, Barcelona, Spain

ARTICLE INFO

Article history:
Received 1 August 2019
Received in revised form
3 January 2020
Accepted 4 January 2020
Available online 7 January 2020

Keywords:
EBPR
nitrite
Polyhydroxyalkanoate (PHA)
Struvite
Recovery

ABSTRACT

Wastewater treatment systems are nowadays evolving into systems where energy and resources are recovered from wastewater. This work presents the long term operation of a demo-scale pilot plant (7.8 m^3) with a novel configuration named as mainstream SCEPPHAR (ShortCut Enhanced Phosphorus and polyhydroxyalkanoate (PHA) Recovery) and based on two sequencing batch reactors (R1-HET and R2-AUT). This is the first report of an implementation at demo scale and under relevant operational conditions of the simultaneous integration of shortcut nitrification, P recovery and production of sludge with a higher PHA content than conventional activated sludge. An operating period under full nitrification mode achieved successful removal efficiencies for total N, P and COD_T (86 ± 12%, 93 ± 9% and 79 ± 6%). In the following period, nitrite shortcut (with undetectable activity of nitrite oxidising bacteria) was achieved by implementing automatic control of the aerobic phase length in R2-AUT using ammonium measurement and operating at a lower sludge retention time. Similar N, P and COD_T removal efficiencies to the full nitrification period were obtained. P-recovery from the anaerobic supernatant of R1-HET was achieved in a separate precipitator by increasing pH and dosing $MgCl_2$, recovering an average value of 45% of the P in the influent as struvite precipitate, with a peak up to 63%. These values are much higher than the typical values of sidestream P-recovery (12%). Regarding PHA, a percentage in the biomass in the range 6.9–9.2% ($gPHA \cdot g^{-1}TSS$) was obtained.

1. Introduction

The water sector has lately changed the paradigm from wastewater treatment to resource recovery. Hence, wastewater treatment plants (WWTPs) are nowadays known as water resource recovery facilities (WRRFs). The major aim of these facilities is to go one-step beyond wastewater treatment and is related to the recovery of energy (for example as biogas, biomethane, or hydrogen) or water and material resources from wastewater (for example as N–P-based fertilisers, bioplastics or cellulose). In this frame, novel WRRFs configurations have been put forward recently.

Phosphorus arises as a perfect candidate in this paradigm shift since it is essential for our society in the production of fertilizers and, thus, for securing food supply. However, the main source of P, the phosphate rock, shows a faster rate of use relative to its formation and, this is why it can be considered as a non-renewable source which, depending on the assumptions taken, is envisaged to be depleted in the next 50–300 years (Ahmed et al., 2015; Cieślik and Konieczka, 2017; Cordell et al., 2011; Theregowda et al., 2019). It is estimated that 3 million tons of P are removed yearly via wastewater treatment in the planet (which represents 15–20% of the global P demand) and, therefore, implementing efficient P-recovery strategies would mitigate the dependence on the phosphate rocks (Mayer et al., 2016)

Enhanced biological phosphorus removal (EBPR) is based on the enrichment of the microbial community in polyphosphate accumulating organisms (PAO), which have a metabolism capable of accumulating P intracellularly as polyphosphate (Poly-P) when alternatively exposed to anaerobic/aerobic (or anoxic) conditions. The fraction of PAO able to accumulate P under anoxic conditions with nitrate/nitrite as electron acceptor are called denitrifying PAO

* Corresponding author.
E-mail addresses: Oriol.Larriba@uab.cat (O. Larriba), Eric.Rovira@uab.cat (E. Rovira-Cal), Zivko.JuznicZonta@uab.cat (Z. Juznic-Zonta), albert.guisasola@uab.cat (A. Guisasola), JuanAntonio.Baeza@uab.cat (J.A. Baeza).

https://doi.org/10.1016/j.watres.2020.115474

Abbreviations

AOB	ammonia oxidising bacteria
A^2/O	anaerobic/anoxic/oxic WWTP configuration
b_{AOB}	apparent decay rate of AOB
BCFS	biological–chemical phosphorus and nitrogen removal process
BMP	biomethane potential
b_{NOB}	apparent decay rate of NOB
BOD	biochemical oxygen demand
CAPEX	capital expenditures
COD	chemical oxygen demand
COD_{CON}	COD consumption in the anaerobic phase for PAO
COD_S	soluble COD
COD_T	total COD
DO	dissolved oxygen
DPAO	denitrifying PAO
EBPR	enhanced biological phosphorus removal
FNA	free nitrous acid
GC	gas chromatography
HRT	hydraulic residence time
IRR	internal rate of return
ISE	ion-selective-electrode
N/D	nitrification/denitrification
NOB	nitrite oxidising bacteria
OPEX	operational expenditures
PAO	polyphosphate accumulating organisms
PHA	polyhydroxyalkanoate
PHB	polyhydroxybutyrate
PHV	polyhydroxyvalerate
PH2MV	polyhydroxy-2-methylvalerate
Poly-P	polyphosphate
P_{REL}	phosphorus release during the anaerobic phase for PAO
P/C	P-release/C-consumption ratio under anaerobic conditions for PAO
rbCOD	readily biodegradable COD
R1-HET	First SBR of the pilot plant, where mostly heterotrophic processes occur
R2-AUT	Second SBR of the pilot plant, where mostly autotrophic processes occur
R3-PRE	Pilot plant reactor for struvite precipitation
R4-INT	Pilot plant vessel for supernatant exchange between R1-HET and R2-AUT
SBR	sequencing batch reactor
SCEPPHAR	Shortcut enhanced phosphorus and polyhydroxyalkanoate recovery
SRT	sludge retention time
TSS	total suspended solids
UCT	University of Cape Town WWTP configuration
V	volume
VER	volume exchange ratio
VFA	volatile fatty acids
VSS	volatile suspended solids
WRRF	water resource recovery facility
WWTP	wastewater treatment plant
μ_{AOB}	apparent growth rate of AOB
μ_{NOB}	apparent growth rate of NOB

(DPAO). Thus, the influent P is accumulated in the biomass purged at the end of the aerobic stage, when the sludge has the maximum amount of Poly-P accumulated. Purging biomass with high P content may have some practical drawbacks since undesired struvite precipitation that clogs pumps and pipes can occur when bio-P sludge is subjected to anaerobic digestion. Decreasing P entrance to the anaerobic digester (for instance, implementing P-recovery) should limit the extent of this uncontrolled precipitation. In fact, struvite recovery has many benefits for the WRRFs, not only for its commercial value but for the reduction of pipe blockage, sludge production, ferric chloride dosage and operation and maintenance costs of the plant (Lizarralde et al., 2019). However, the efficiency of P recovery from the anaerobic digestate is only about 12% of the P entering in the influent (Remy and Jossa, 2015) and therefore alternatives must be found to achieve a more significant percentage of P recovery.

An option to increase the amount of P recovered and to avoid undesired struvite precipitation is the implementation of mainstream P-recovery based on EBPR activity. Some authors have already shown that a significant P extraction from the anaerobic phase of EBPR systems can be maintained at long-term without any deleterious effect on PAO activity (Guisasola et al., 2019). Some examples are the BCFS® process (Biological–chemical phosphorus and nitrogen removal) (Meijer et al., 2001; van Loosdrecht et al., 1998) or other reports (Baeza et al., 2017; Kodera et al., 2013; Shi et al., 2012; Valverde-Pérez et al., 2015). A common conclusion of these works is that up to 60% of the influent P could be recovered at the end of the anaerobic phase under well-controlled conditions.

Anaerobic extraction of the supernatant can lead to another advantage in terms of resource recovery, since it opens the door to anaerobic purging of EBPR sludge. PAO accumulate polyhydroxyalkanoate (PHA) under anaerobic conditions from the volatile fatty acids (VFA) taken up. This PHA would be used as energy and carbon source in a posterior phase under aerobic/anoxic conditions. Purging at the end of the anaerobic phase results in biomass with the highest PHA content of the whole operation, whereas the conventional aerobic purging results in a purge with low PHA content. Sludge rich in PHA shows two potential advantages: i) it can be used as a precursor for bioplastics production after its extraction and ii) if sent to the anaerobic digester, this sludge would have a higher potential methane production due to its higher PHA content (Chan et al., 2020; Huda et al., 2016; Wang et al., 2016).

Regarding N removal, the nitrite pathway approach, i.e. nitritation ($NH_4^+ \rightarrow NO_2^-$) followed by denitritation ($NO_2^- \rightarrow N_2$), has been reported to have advantages when compared to conventional nitrification and denitrification processes (Türk and Mavinic, 1987): i) 25% lower oxygen consumption for N oxidation, thus reducing aeration costs and also lowering the carbon footprint of a WWTP, ii) up to 40% lower COD requirement for denitrification and iii) faster denitrification rate (1.5–2 times), thus requiring smaller anoxic basin. The nitrite pathway has already been reported with low strength municipal wastewater (Guo et al., 2009; Ma et al., 2009; Yang et al., 2007), and also integrated with EBPR (Marcelino et al., 2011). Moreover, nitrite has been also reported as a good electron acceptor for DPAO (Tayà et al., 2013).

Nitritation, the first step of the nitrite pathway, is achieved by creating conditions where nitrite oxidising bacteria (NOB) are eliminated from the system while ammonia oxidising bacteria (AOB) are retained. Mathematically, equation (1) should be satisfied in order to eliminate NOB while retaining AOB:

$$\mu_{NOB} - b_{NOB} < SRT^{-1} < \mu_{AOB} - b_{AOB} \quad (1)$$

where μ_{NOB} and μ_{AOB} are the apparent growth rates of NOB and AOB, respectively, b_{NOB} and b_{AOB} the apparent decay rates of these populations, and SRT the sludge retention time. Most of the strategies enabling the nitrite pathway involve manipulating μ_{NOB} and μ_{AOB} such that equation (1) is satisfied. In most cases, it is inevitably to reduce both μ_{NOB} and μ_{AOB} but incurring stronger reductions in μ_{NOB}. A common strategy reported in the literature to obtain NOB washout is to decrease the dissolved oxygen (DO) setpoint (Aslan et al., 2009; Blackburne et al., 2008; Jiang et al., 2019; Jianlong and Ning, 2004; Pollice et al., 2002) since it is widely accepted that AOB have higher affinity with oxygen than NOB. The drawback of operating at low DO value is that higher N_2O emissions may occur (Massara et al., 2018, 2017).

Hence, this work proposes a novel WRRF configuration named as mainstream SCEPPHAR (ShortCut Enhanced Phosphorus and PHA Recovery), which is one of the novel technologies involved in the SMART-Plant project (www.smart-plant.eu). The whole SMART-Plant project aims to prove the feasibility of novel wastewater treatment technologies at demo pilot-scale towards a circular economy scenario, not only to treat wastewater, but also to recover resources. SCEPPHAR configuration redesigns the two-sludge system proposed by Marcelino et al. (2011) to include in the mainstream resource recovery (struvite and PHA-rich sludge). The system is based on two sequential batch reactors (SBR): one mainly heterotrophic (R1-HET) performing EBPR under alternating anaerobic/anoxic/aerobic conditions and another mainly autotrophic (R2-AUT) in charge of ammonia oxidation to nitrite (complete nitritation).

This work presents the critical assessment for long-term operations of a demo-scale mainstream SCEPPHAR pilot plant treating real wastewater from a municipal WWTP, showing the resource recovery possibilities of this novel configuration. To the best of our knowledge, this is the first report in the literature of an implementation at demo scale and under relevant operational conditions of the integration in a mainstream configuration of nitrite pathway, P-recovery and production of sludge with increased PHA content.

2. Materials and methods

2.1. SCEPPHAR pilot plant configuration

The demo-scale pilot plant was located in the municipal WWTP of Manresa (Barcelona, Spain). Fig. 1 shows the process diagram of the pilot plant, which includes: i) R1-HET anaerobic/anoxic/aerobic SBR (V = 2500L) for heterotrophic processes, ii) R2-AUT aerobic SBR (V = 2500L) for autotrophic nitrification, iii) R3-PRE reactor (V = 150L) for struvite precipitation, and iv) R4-INT vessel (V = 2500L) for interchanging supernatants between R1-HET and R2-AUT. The pilot plant operated with 70% of volume exchange ratio (VER), i.e. 1750 L of wastewater were treated per cycle. Table 1 summarizes the main operational parameters for the three periods reported: start-up, complete nitrification and nitrite pathway. Hydraulic residence time (HRT) is calculated considering both R1-HET and R2-AUT volume, and the independent SRT fixed for each reactor is also included.

R1-HET and R2-AUT were inoculated with activated sludge from the Manresa WWTP (anoxic/aerobic configuration with N/D but no EBPR) and R1-HET was bioaugmented with PAO-enriched sludge from an EBPR pilot plant (Rey-Martínez et al., 2019). The wastewater used was the effluent of the primary settler of the Manresa WWTP with the average composition shown in Table 2.

Each of the cycles follows the next operational sequence: the process starts with the influent feeding to R1-HET. Then, an anaerobic phase takes place and PAO uptake organic matter, release P, and accumulate PHA. An anaerobic purge is performed and, after settling, the supernatant of the reactor, which is rich in phosphates and ammonia, is sent to R4-INT. Then, 150 L of R4-INT are sent to R3-PRE for P precipitation as struvite. The rest of content of R4-INT is transferred to R2-AUT, where ammonia is oxidised to nitrate or nitrite (depending on the period). After settling in R2-AUT, the supernatant is returned to R1-HET for an anoxic phase. During this R1-HET phase, denitrifying PAO (DPAO) perform P-uptake using nitrite/nitrate as electron acceptor. Finally, an aerobic phase is required to complete P-uptake. After settling, the supernatant is discharged to the effluent and the cycle starts again. The complete sequence of the pilot-plant when operating with a cycle length of 12 h is detailed in Table 3, while the 8 h cycle used during part of Period I is reported in the supplementary information (Table S1).

2.2. Pilot plant monitoring and control system

R1-HET, R2-AUT and R4-INT had on-line monitoring of level (Endress Hauser), which was essential for the automation of the interexchange steps between the reactors. R1-HET and R2-AUT were monitored with DO (Hach Lange), temperature (Pt1000, Axiomatic), pH and oxidation reduction potential (Hach Lange). R2-AUT had also an on-line ion-selective-electrode (ISE) for ammonia/nitrate (Hach Lange) for the automation of the aeration phase control length. R3-PRE was monitored with a pH sensor (Hach Lange). Aeration flow of the reaction vessels was monitored with gas rotameters (Iberfluid). R1-HET, R2-AUT and R3-PRE were stirred (Milton Roy Mixing) during the reaction phases. Centrifugal pumps (Grundfos) were used for water interchange, and dosing pumps (Seko) for sludge purge and dosage of Mg and acetic acid. All the mechanical equipment and monitoring systems were connected to an industrial computer (PPC-3170, Advantech) through a data acquisition system (PCI-1711 I/O card, Advantech). The software Addcontrol developed by the research group was used for automating all the operation, monitoring and control. DO was controlled by manipulating the aeration flow-rate through electric control valves (Type 3241/3374, Samson Instruments) based on the DO measurement and a proportional-integral algorithm programmed in the control system. DO setpoint in the aerobic phases of R1-HET and R2-AUT was always maintained at 3 mg L^{-1}.

2.3. Chemical analysis

All the samples for the determination of soluble compounds were filtered with a 0.22 μm filter (Millipore) before the analysis. P was measured with a phosphate analyser (115 VAC PHOSPHAX sc, Hach-Lange) based on the Vanadomolybdate yellow method samples. Ammonium nitrogen was analysed with an ammonium analyser (AMTAXsc, Hach Lange), based on the potentiometric determination of ammonia. Nitrite and nitrate were analysed with Ion Chromatography (DIONEX ICS-2000).

Volatile suspended solids (VSS) and total suspended solids (TSS) in mixed liquor were analysed according to Standard Methods (APHA, 1995). COD was analysed by using Lovibond kits (COD Vario Tube Test LR and COD Vario Tube Test MR) and the MD100 Lobivond spectrophotometer. Soluble COD (COD_S) was measured with samples filtered through 0.22 μm filters, while total COD (COD_T) was not filtered. The PHA content in the biomass was measured as follows: 0.6 mL of formaldehyde was added to each sample to stop the biological reactions and then the sample was lyophilised. The PHA was extracted from lyophilised samples using hexane and butanol according to the method of Werker et al. (2008). Subsequently, the PHA was determined with a GC (Agilent Technologies 7820A) as described in Montiel-Jarillo et al. (2017). The standards used were 3-hydroxybutyric acid and 3-hydroxyvaleric acid copolymer for polyhydroxybutyrate (PHB) and

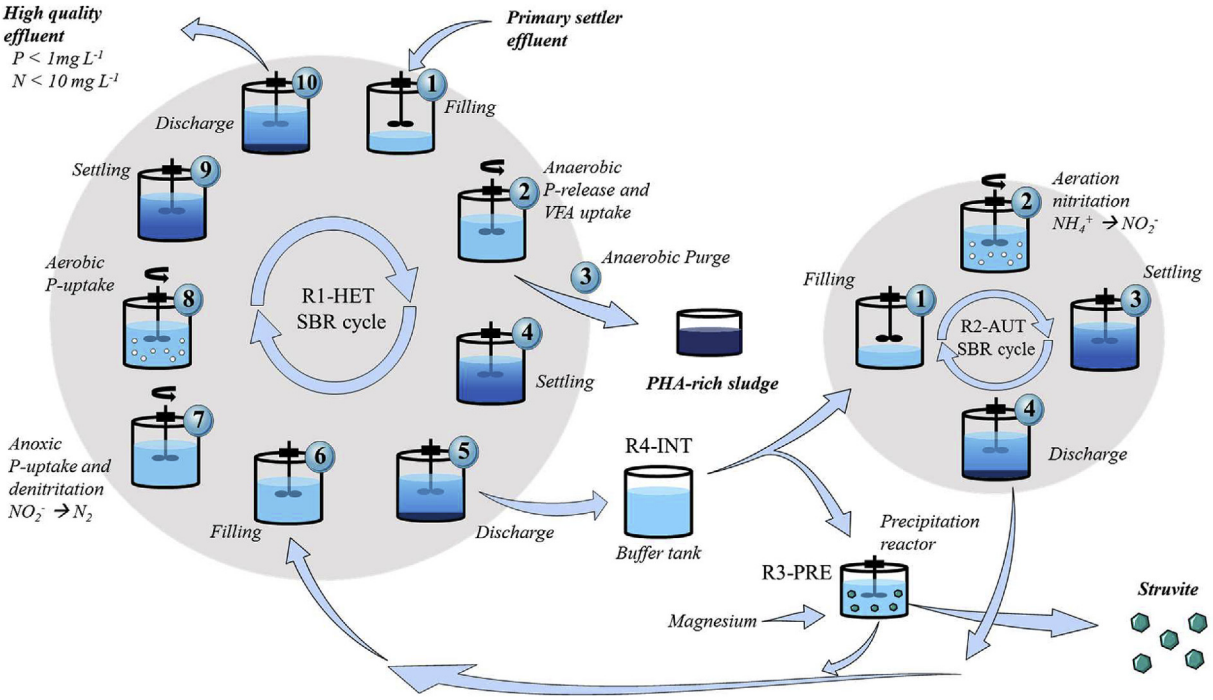

Fig. 1. Schematics of the SCEPPHAR configuration as implemented in the demosize pilot-plant.

Table 1
Main operational parameters used for each period.

Period		Days	Cycle length (h)	HRT (d)	SRT (d) R1-HET	SRT (d) R2-AUT	Aerobic length control
I	Start-up		8–12	1–1.5	15	15	N
II	Complete nitrification	0–225	12	1.5	10	12	N
III	Nitrite shortcut	291–439	12	1.5	10	5–7	Y

Table 2
Average composition of the influent of the pilot plant (effluent of the primary settler of the full-scale WWTP of Manresa).

Compound	Concentration	Units
PO_4^{3-}-P	4.2 ± 1.1	mgP·L^{-1}
NH_4^+-N	40 ± 11	mgN·L^{-1}
NO_2^--N	0.1 ± 0.1	mgN·L^{-1}
NO_3^--N	1.3 ± 0.7	mgN·L^{-1}
COD_T	228 ± 81	mgCOD·L^{-1}
COD_S	136 ± 39	mgCOD·L^{-1}
Temperature	20 ± 6	°C

polyhydroxyvalerate (PHV) and 2-hydroxycaproic acid as standard for polyhydroxy-2-methylvalerate (PH2MV).

2.4. Batch experiments

2.4.1. Sampling and monitoring

The biomass used in all the batch experiments was withdrawn from the pilot plant at the end of a cycle. Then, biomass was washed three times with tap water and was left overnight with magnetic stirring and aeration in order to consume the remaining COD and to achieve endogenous conditions at the beginning of the experiments.

The batch experiments were conducted in a 2 L vessel with on-line pH, DO and temperature monitoring as in (Guisasola et al., 2007). The probes, pH (Sentix 81, WTW) and DO (Cellox 325, WTW), were connected to a multiparametric device (INOLAB 3, WTW) which in turn was connected via RS232 to a computer with an own data acquisition software developed in Visual Basic.

In every experiment, 40 mL samples were extracted every 30min for the analytical tests. The samples were processed with a centrifuge (Beckman Coulter, Avanti J-20 XP) and filtered through 0.22 μm pore diameter filters (Millipore).

2.4.2. PAO/DPAO activity batch experiments

The PAO/DPAO activity tests were comprised of three sequential phases mimicking the cycle of R1-HET: an anaerobic phase (180 min), followed by an anoxic phase (60 min) and a final aerobic phase (120 min). The first anaerobic phase was obtained by sparging N_2 gas. At the beginning of the experiment, a pulse of nutrients was added so that the concentrations were: phosphorus 10 mg PO_4^{3-}-P L^{-1} (KH_2PO_4), acetic acid 150 mg L^{-1} and ammonium 20 mg NH_4^+-N L^{-1} (NH_4Cl). The anoxic conditions were obtained by adding at time 180 min a single dose of nitrite or nitrate so that the concentrations were: nitrite 15 mg NO_2^--N L^{-1} ($NaNO_2$) or nitrate 15 mg NO_3^--N L^{-1} ($NaNO_3$). The nitrite/nitrate added was equivalent to the ammonium that would have been oxidised during the nitrification phase in R2-AUT of the pilot plant. Finally, the aerobic phase was accomplished by sparging air, maintaining a DO between 2 and 5 mg L^{-1}.

2.4.3. Nitrification activity experiments

Nitrification activity tests comprised two aerobic phases of

Table 3
Typical configuration of the four reactors of the pilot plant with a 12 h cycle length.

R1-HET (heterotrophic SBR)		**R2-AUT** (autotrophic SBR)	
Time (min)	Phase	Time (min)	Phase
0–37	Feeding from influent	37–358[1]	Aerobic
37–355	Anaerobic	358[1]–413	Settling
355–360	Purge	413–441	Extraction to R1-HET
360–385	Settling	441–465	Feeding from R4-INT
385–413	Extraction to R4-INT	465–470	Purge to R1-HET
413–441	Feeding from R2-AUT + R3-PRE	470–37[2]	Idle
441–541	Anoxic		
541–661	Aerobic		
661–691	Settling		
691–720	Extraction to effluent		
R3-PRE (precipitation reactor)		**R4-INT** (interchange vessel)	
Time (min)	Phase	Time (min)	Phase
385–413	Settling	385–413	Feeding from R1-HET
413–425	Extraction to R1-HET	413–425	Idle
425–435	Feeding from R4-INT	425–435	Extraction to R3-INT
435–385[2]	Precipitation: Mg^{2+} addition	435–465	Extraction to R2-AUT
		465–385[2]	Idle

[1] Maximum value (the real value depends on the control of the aeration phase length).
[2] Time of the following cycle.

120 min each, with a DO between 2 and 5 mg L^{-1}. At the beginning of the experiment, ammonium (NH_4Cl) was added so that an initial concentration of 15 mg NH_4^+-N L^{-1} was obtained. If required, a second aerobic phase was planned with a pulse of nitrite ($NaNO_2$).

2.5. Calculations

The observed production and consumption rates of the studied variables were calculated as follows:

$$Production\ or\ consumption\ rate = \frac{\Delta C}{t_f - t_o} \quad (2)$$

$$Specific\ production\ or\ consumption\ rate = \frac{\frac{\Delta C}{t_f - t_o}}{VSS} \quad (3)$$

Where ΔC is the concentration difference between the beginning and the end of the period with linear behaviour in mg L^{-1}, t_o and t_f are the initial and final time in minutes, and VSS concentration is in mg L^{-1}.

Furthermore, the ratio P-release/C-consumption (P/C) during the anaerobic phase was calculated as a PAO activity indicator:

$$P \Big/ C\left(\frac{molP}{molC}\right) = \frac{\frac{P_{REL}}{M_P}}{\frac{COD_{CON}}{32}} \quad (4)$$

Where P_{REL} is the phosphorus release during the anaerobic phase in mg PO_4^{3-}-P L^{-1}, M_P is the P molecular weight (30.97 g/mol), COD_{CON} is the COD consumption in the anaerobic phase in mgO_2 L^{-1}, and 32 is the factor gO_2/C mol for acetate.

Total N removal was calculated as ammonium in the influent minus the sum of the nitrogen species measured in the effluent as ammonium, nitrite and nitrate.

2.6. Economic assessment

The economic feasibility of the mainstream SCEPPHAR configuration was evaluated and compared to a traditional A^2/O configuration for a time span of 30 years. The detailed methodology and results can be found in the Supplementary Information. The major design assumptions were: i) primary and secondary settlers are not needed for the SCEPPHAR plant while they are considered for the A^2/O plant, ii) three independent SCEPPHAR process lines are needed to guarantee the continuous operation and to ease the maintenance, and iii) just one warehouse spare equipment unit (i.e. blower and pumps) for all process lines is purchased as a backup. Incomes were derived from the net production of electricity (i.e. biogas) and wastewater tariff. The cash-flow relative to struvite was negligible compared to the other costs. PHA recovery incomes were excluded because of the low PHA content, but the increase in biogas production due to the PHA concentration in the sludge was considered. External carbon addition was not accounted since the biochemical oxygen demand (BOD) content was considered high enough to promote both N and P removal.

3. Results

3.1. Period I. Preliminary results and operational changes during the start-up

In a first start-up (Period I), the system was operated for more than three months with a configuration of 8 h per cycle (Table S1). Ammonia was fully oxidised since R2-AUT was enriched in nitrifying organisms. However, EBPR activity was not detected, indicating the absence of PAO in R1-HET. The low COD present in the influent (150 ± 40 mgCOD·L^{-1}) was a clear bottleneck for the implementation of EBPR. In addition, specific batch tests in R1-HET demonstrated that COD remained almost constant during the anaerobic phase and that no VFA were detected, revealing that besides the low COD content there was a lack of COD fermentation to VFA. To enhance fermentation and to increase the VFA availability for PAO, the anaerobic phase was increased from 3 to 6 h and the whole cycle length was extended from 8 to 12 h using the configuration reported in Table 3. After several weeks with this extended cycle length, PAO activity remained very low. Finally, it was decided to add an external carbon source (acetic acid, additional concentration of 100 mg COD·L^{-1}) at the beginning of the anaerobic phase. Fig. S1 compares an example of the anaerobic P release obtained in two different cycles without and with VFA addition.

Considering the low COD available in the wastewater used and the results obtained during Period I, the SCEPPHAR pilot plant was operated from that moment onwards with a cycle configuration of 12 h and with an automated dosage of acetic acid (to increase the COD concentration by 100 mgCOD·L^{-1} at the beginning of the anaerobic phase in R1-HET). After this operational change, R1-HET was progressively enriched in PAO and EBPR activity increased, promoting stable and good removal for P and N.

3.2. Period II. Stable operation of the SCEPPHAR pilot plant with complete nitrification

This section reports the results obtained during the long-term monitoring of Period II, when the pilot plant was operated under complete nitrification mode and had good PAO activity. Fig. 2 shows the ammonium, phosphate and COD_S input/output profiles of the pilot plant once the PAO activity was enhanced and Table 4 shows the average solids concentrations. During the days 0–175, the effluent P was consistently below the discharge limit, with an average of 0.2 ± 0.1 mgPO_4^{3-}-P·L^{-1}. Ammonium oxidation was almost complete, with average effluent concentration of 1.9 ± 2.5 mg NH_4^+-N·L^{-1}. Nitrite, nitrate and TN average concentration in the effluent were 0.5 ± 1.2 mg NO_2^--N·L^{-1}, 3.7 ± 0.9 mg NO_3^--N·L^{-1} and 5.2 ± 3.6 mgTN·L^{-1}. Hence, the pilot plant was accomplishing its main objective, which was to meet legal discharge limits for the Manresa WWTP (P < 1 mgP·L^{-1}, NH_4^+-N < 4 mgN·L^{-1} and TN < 10 mgN·L^{-1}, (EEC Council, 1991)). The removal efficiencies during Period II for total N, P and COD_T were 86 ± 12%, 93 ± 9% and 79 ± 6%. Ammonia oxidation started to decrease on day 180, because of a significant decrease in temperature (Fig. S2) and because the aeration phase in R2-AUT was limited to 3 h.

Concerning to COD_S, Fig. 2C shows the low influent concentration and high variability (136 ± 39 COD_S·L^{-1}), the values at the effluent of 31 ± 14 mg COD_S·L^{-1} and removal efficiencies higher than 75%. The lack of COD in this wastewater was alleviated by the addition of the 100 mgCOD·L^{-1} of acetic acid. The need of this addition was corroborated in some cycles (days 180–195) where a pump malfunctioning led to the absence of this extra VFA and resulted in a lower P-removal.

Fig. 3 shows an example of a cycle operation, obtained at day 139 of operation, when the system was under stable operation with complete nitrification. The cycle started with the feeding of 1750 L of wastewater (step 1 for R1-HET in Fig. 1). The influent wastewater in this cycle contained 3.8 mgPO_4^{3-}-P·L^{-1} and 31.3 mgNH_4^+-N·L^{-1}. Considering the concentrations in the remaining mixed liquor in R1-HET before the feeding (30% of the reactor volume) and a possible concentration similar to that of the end of this cycle (around 0 mg PO_4^{3-}-P·L^{-1} and 0 mgNH_4^+-N·L^{-1}), the initial concentrations in R1-HET after the feeding should have been around 2.7 mgPO_4^{3-}-P·L^{-1} and 21.8 mg NH_4^+-N·L^{-1}. The first measurements (t = 0.633 h) showed that the theoretical ammonium concentration (21.8 mgNH_4^+-N·L^{-1}) agreed with the measured value (22.8 mg NH_4^+-N·L^{-1}), but did not agree for phosphate. The experimental measurement was 13.2 instead of 2.7 mgPO_4^{3-}-P·L^{-1}. This increase was related to the length of the feeding phase (38 min): PAO could release P linked to the uptake of the VFA available in the wastewater.

During the following anaerobic phase (step 2 for R1-HET) P concentration increased linked to VFA consumption by PAO, reaching 34.8 mgPO_4^{3-}-P·L^{-1} at the end of this phase (an increase of 9.2 times the initial wastewater concentration). On the other hand, ammonium concentration remained almost constant during this anaerobic phase, with 22.3 mg NH_4^+-N·L^{-1} at the end of this phase. Then, biomass was purged (step 3) to maintain the SRT around 10d and the stirring was turned off for biomass settling. After settling (step 4), the supernatant of R1-HET (70% of the volume) was transferred to R4-INT (step 5). In the following step 6, R1-HET received the supernatants of R2-AUT (containing the water of the previous cycle after nitrification) and R3-PRE (150L). After this water interchange, the concentration of ammonium (Fig. 3) at the beginning of the anoxic phase decreased significantly down to 8.5 mg NH_4^+-N·L^{-1}, as the content of R1-HET (30% remaining after settling) was diluted with the nitrified water from R2-AUT with ammonium concentration around 0 mg NH_4^+-N·L^{-1}. Phosphate also decreased to 27.1 mgPO_4^{3-}-P·L^{-1} due to the added effect of three different processes: i) struvite precipitation in R3-PRE that reduced the concentration of phosphate in the supernatant of this reactor, ii) occurrence of some P-uptake in R2-AUT and iii) DPAO activity during the filling of R1-HET from R2-AUT, as nitrate content in this exchanged water can be used as electron acceptor for P-uptake.

During the rest of the anoxic phase (step 7), the remaining nitrate could be used as electron acceptor for DPAO activity. In the cycle presented, initial nitrite/nitrate concentration was low, as it was almost depleted during the previous feeding phase, and hence anoxic P-uptake was low. Regarding the other monitored variables, ammonium concentration did not change significantly, and a slight COD consumption was observed. Finally, in the following aerobic phase (step 8), P-uptake was fast, reaching 0.06 mgPO_4^{3-}-P·L^{-1} at the end of the phase. Ammonium was fully oxidised and COD_S was only 16 mgCOD·L^{-1} at the end of this phase. Finally, aeration and stirring were turned off for the last settling (step 9) and discharge (step 10), where a very high quality effluent was obtained, fully accomplishing discharge limits.

Regarding R2-AUT, it received the anaerobic supernatant of R1-HET through the buffer R4-INT (step 1 for R2-AUT). The aerobic phase (step 2) was designed for ammonia oxidation to nitrate, and it accomplished its objective, reducing the ammonium concentration from 17.3 to 0 mg NH_4^+-N·L^{-1} and increasing the concentration of nitrate up to 17.6 mg NO_3^--N·L^{-1} during its 2 h of duration (Fig. 3). The rest of the cycle time in R2-AUT was devoted to idle, settling, discharge, filling and purge (steps 3, 4, 1). Fig. 3 also reveals some P-removal in R2-AUT, probably due to the aerobic/extended-idle configuration used in this reactor. The presence of PAO in this configuration is attributed to the non-aerated extended-idle phase acting as a post anaerobic zone (Wang et al., 2012).

Finally, R3-PRE receives 150 L of anaerobic supernatant from R4-INT. This stream has a higher P content than the influent and a similar high content of ammonium. Phosphate precipitation took place in this reactor when pH was increased up to 8.5 by air sparging for CO_2 stripping and the addition of 19 mg Mg^{2+}·L^{-1} as concentrated solution of $MgCl_2$. Typically, P concentration in R3-PRE decreased around 65%–75% at the end of the phase. The supernatant of this reactor was also sent to R1-HET during step 6 (Fig. 1).

3.3. Period III. Achieving nitrite-shortcut in the SCEPPHAR configuration

Before moving to shortcut nitrogen removal, the pilot plant was stopped for maintenance and some valves and pumps were replaced because of clogging issues. Hence, Period III starts at day 275 after a new inoculation. The input/output profiles for phosphate and ammonium during this period are shown in Fig. 4, the average solids concentration are reported in Table 4 and finally Fig. S3 shows the temperature profile in R1. The plant showed complete nitrification on day 341 with good nutrient removal performance. The system recovered a similar removal performance to that observed during Period II with an effluent below discharge limits. Fig. S4 shows a fully monitored cycle on day 362. The profiles during this batch cycle were also similar to those obtained on day

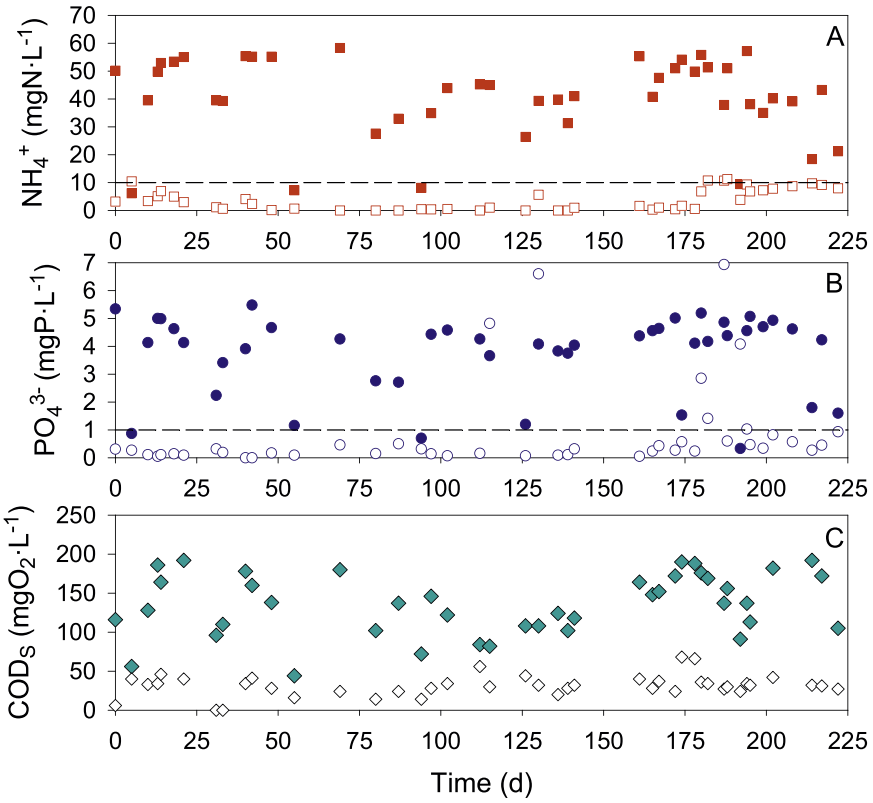

Fig. 2. Period II. Inlet/outlet profiles for ammonium (A), phosphate (B) and soluble COD (C). Filled symbols: inlet, void symbols: outlet, dash line: discharge limit for TN and P.

Table 4
Average solids concentrations in R1-HET and R2-AUT during all the operational periods.

Operational period (days)	Reactor	VSS (gVSS·L^{-1})	TSS (gTSS·L^{-1})
Period II	R1-HET	1.44 ± 0.18	1.70 ± 0.22
	R2-AUT	3.30 ± 0.80	4.09 ± 1.00
Period III	R1-HET	2.03 ± 0.18	2.48 ± 0.12
	R2-AUT	2.15 ± 0.12	2.80 ± 0.16

139 (Fig. 3): only slightly lower P-release activity was observed during the anaerobic phase.

Once the system was stable (day 363), two operational changes were implemented to decrease NOB activity in R2-AUT: i) real-time control of the length of the aerobic phase using the on-line ammonium measurement and ii) operating at lower SRT. The proposed strategy does not require operating at a low DO value to achieve nitritation and, hence, the DO setpoint was maintained at 3 mg L^{-1}, avoiding a potential increase of N_2O emissions reported at lower DO (Massara et al., 2018, 2017).

Fig. 5A shows an example of the ammonium and nitrate monitored in some cycles of R2-AUT on day 365, two days after implementing the aerobic length control strategy. Ammonium was oxidised during the aerobic phase linked to the increase of nitrate concentration, measured by the same on-line sensor. Aeration and stirring were automatically turned off when the ammonium concentration decreased below 3 mgNH_4^+-N·L^{-1}. However, stirring was not stopped in the cycles shown in Fig. 5A to have representative values of the monitored variables. During the non-aerated phase, ammonium remained almost constant, probably related to the detection level of the on-line ISE analyser, while nitrate slightly increased due to some nitrite oxidation, probably because of oxygen surface transfer due to the stirring. Nevertheless, this problem was not observed in the conventional operation of the plant.

Fig. 5B shows a batch experiment conducted on day 378, 15 days after implementing the control strategy. During the first part of the experiment, ammonium was oxidised at a rate of 5.7 mgNH_4^+-N·L^{-1}·h^{-1}, nitrite was accumulated at 3.2 mgNO_2^--N·L^{-1}·h^{-1} and nitrate was produced at 2.7 mgNO_3^--N·L^{-1}·h^{-1}. These values indicated that AOB activity (oxidation of ammonium) duplicated the activity of NOB (production of nitrate), leading to accumulation of nitrite. Moreover, in the second part of the experiment, after the addition of an excess of nitrite, NOB activity slightly decreased to 2.2 mgNO_3^--N·L^{-1}·d^{-1} instead of increasing. This indicated that NOB were the limiting step and that the first actions towards decreasing NOB activity were positive.

After a month of implementing the control strategy, NOB activity was undetectable and the nitrite-shortcut SCEPPHAR configuration was effectively obtained. Fig. 6 shows two examples of pilot plant cycles obtained on days 410 and 439 of operation. Ammonium in R2-AUT was completely oxidised to nitrite, without detecting nitrate and matching nitrite formation to ammonia oxidation. The aeration phase length was shorter on day 439 since the controller adapts this length automatically. Fig. S5 shows an example of a batch test with R2-AUT biomass on day 419, where a high ammonium concentration was added at DO setpoints of 1, 2 and 3 mgO_2·L^{-1}. Nitrate was not observed at any DO setpoint, indicating the lack of NOB activity.

Returning to the experiments on Fig. 6, the nitrite-rich effluent of R2-AUT entered the anoxic phase of R1-HET. Nitrite was not detected in the first sample of the anoxic phase because the feeding time of 28 min was enough to reduce the available nitrite by DPAO, as already observed for nitrate in the previous cycles. No additional

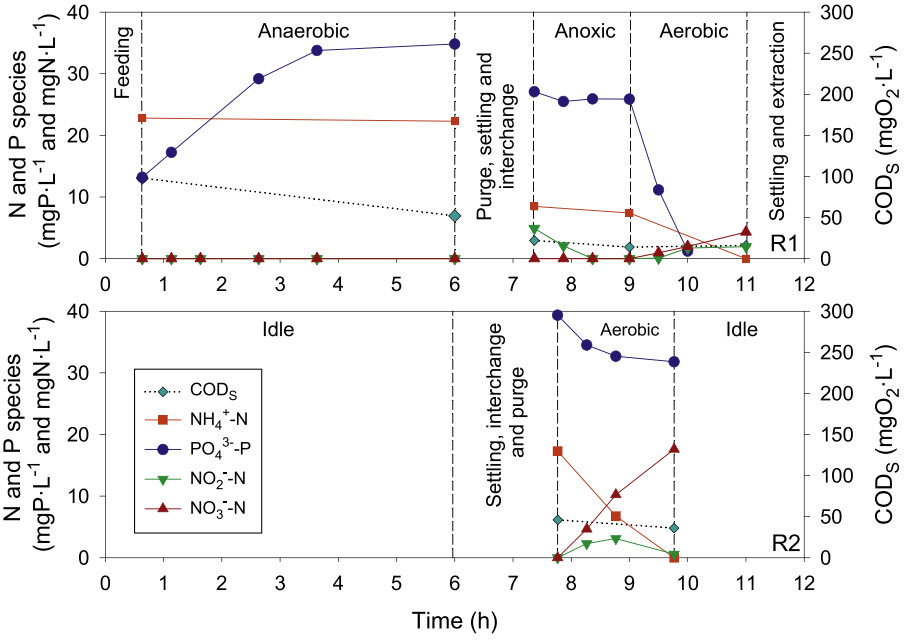

Fig. 3. Period II. Typical SCEPPHAR cycle with complete nitrification obtained at day 139 of operation for R1-HET and R2-AUT.

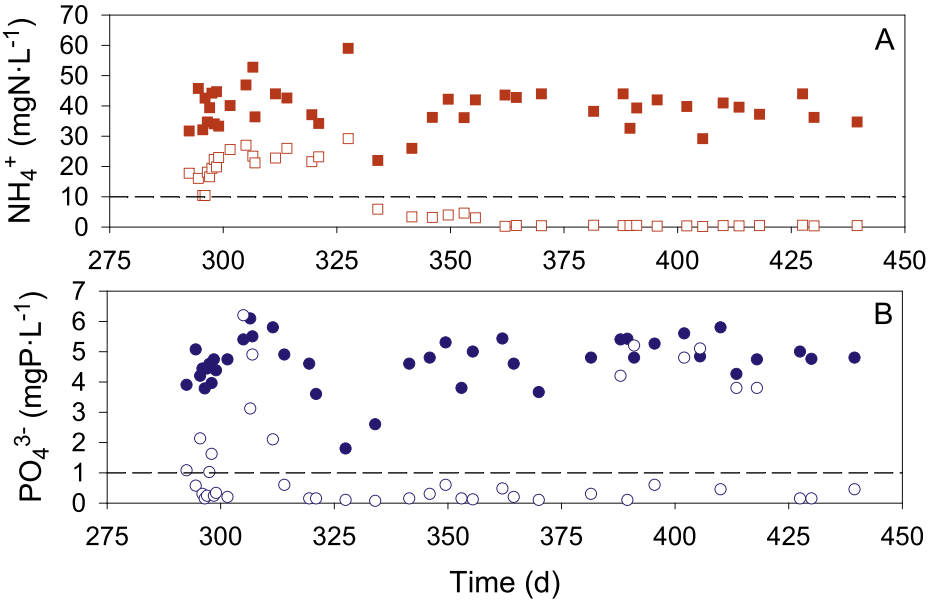

Fig. 4. Period III. Inlet/outlet profiles for ammonium (A) and phosphate (B). Filled symbols: inlet, void symbols: outlet, dash line: discharge limit for TN and P.

nitrite-based DPAO activity was observed during the rest of anoxic phase due to the lack of nitrite. However, nitrite DPAO were very active as demonstrated in the specific batch experiment shown in Fig. 7, where a nitrite reduction rate of 0.072 mg $N-NO_2^- \cdot g^{-1}$ $VSS \cdot min^{-1}$ was observed. This high nitrite DPAO activity indicates that a fraction of P was uptaken in the anoxic feeding phase of R1-HET. The most significant result of the SCEPPHAR configuration in Period III was the successful P-removal using N-removal via nitrite. Moreover, some P-uptake was also observed in R2-AUT, similarly to Period II, and showing that the nitrite shortcut did not affect potential PAO presence in R2-AUT. Regarding the overall removal efficiencies during Period III, they were similar to Period II: 82 ± 11% for total N, 94 ± 12% for P and 80 ± 7% for COD_T.

Tables 5 and 6 show the main parameters of R1-HET and R2-AUT in the four cycles presented in this manuscript. The maximum specific rates for conventional EBPR processes (i.e. COD uptake and P-release) were obtained for the case with full nitrification. However, under nitrite-shortcut mode the P-removal efficiencies were not affected in spite of the lower specific rates. The nature of the influent COD was very diverse: from complex COD to VFA. Thus, simultaneous fermentation and COD uptake could be occurring under anaerobic conditions. The P/C values were quite high for being a real wastewater, probably due to the acetic acid amendment. Regarding the N-related processes, the specific ammonium oxidation rate increased during time and it was higher when nitrite shortcut was applied, probably also due to the lower SRT used (5-

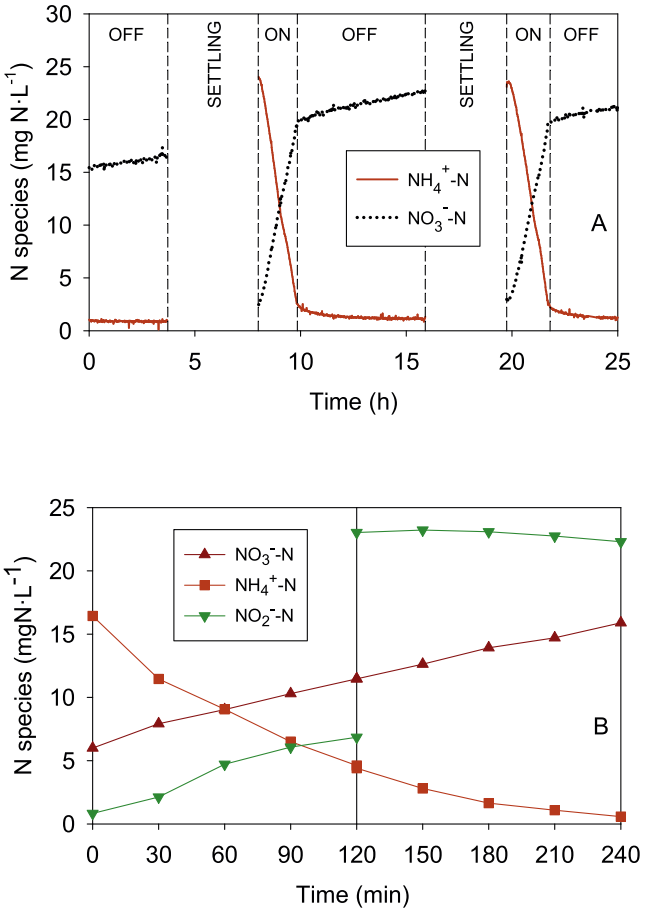

Fig. 5. A) Example of on-line ammonium and nitrate measurements in R2-AUT during some cycles on day 365 of operation, two days after implementing the aeration length control. The DO control loop was activated during the ON periods. B) Batch experiment for evaluating the decrease of NOB activity, performed with biomass obtained from R2-AUT on day 378 of operation.

7d) that led to lower biomass concentration (Table 4). The ratio of nitrate with respect to the initial ammonium was close to one in the complete nitrification cycles, while the ratio of nitrite versus initial ammonium was close to one in the two cycles reported with nitrite-shortcut.

3.4. Resource recovery

The main purpose of the mainstream SCEPPHAR configuration was to examine the feasibility of recovering resources from the wastewater besides obtaining a good effluent quality. Regarding the recovery of P as struvite, the typical values obtained in R3-PRE showed P-precipitation to be in the range 65–90% depending on the specific cycle and precipitation conditions. Magnesium was added in the range 1–1.5 $molMg^{2+}\cdot mol^{-1}P$: a fixed amount of Mg^{2+} was dosed but the P concentration at the beginning of the precipitation phase in R3-PRE was variable. P-recovery in R3-PRE was feasible due to the increased concentration of P obtained at the end of the anaerobic phase with respect to the influent. The average concentration of P in R3-PRE was 6.2 ± 2.4 times the influent concentration with a maximum increase of 9.2 times in the cycle of day 139. An average 45% of the P in the influent could be recovered as struvite following the next considerations: a typical precipitation of 70% of the initial P in R3-PRE, an influent of 1750L of wastewater with 4 $mgPO_4^{3-}\text{-}P\cdot L^{-1}$ and that 150L of anaerobic supernatant with 30 $mgPO_4^{3-}\text{-}P\cdot L^{-1}$ were sent to R3-PRE. When considering the best scenario (day 139), a supernatant of 35 $mgPO_4^{3-}\text{-}P\cdot L^{-1}$, influent 3.8 $mgPO_4^{3-}\text{-}P\cdot L^{-1}$ and 80% of precipitation, the recovery increased up to 63%.

The biomass extracted at the end of the anaerobic phase has a higher PHA content than the typical purge obtained at the end of the aerobic phase. PHA analyses in a conventional cycle of the pilot plant showed percentages of PHA in the biomass ($gPHA\cdot g^{-1}TSS$) of 3.1% and 6.9% at the start and end of the anaerobic phase. Batch experiments with excess of VFA and left overnight increased PHA content from 0.7% to 9.1%, which is the maximum value measured with this sludge. This value would be obtained by adding an excess of VFA in all or some of the cycles in the pilot plant.

3.5. Economic assessment

This section reports the main results obtained for the economic evaluation, which is detailed in the Supplementary Information. The net present value for SCEPPHAR and A^2/O were estimated at 58.2 and 63.4 M€, respectively. Considering a wastewater tariff of 0.73 €/m^3, the internal rate of return (IRR) was very high for SCEPPHAR and A^2/O: 21% and 29%, respectively. The slightly better outcome for the A^2/O technology was mainly due to its lower capital expenditures (CAPEX) (15.9 M€) compared to SCEPPHAR (21.8 M€), due to the discontinuous nature of the SBR operation. The cost advantage of missing settler units in SCEPPHAR was off-set by the higher total tank volumes and mixing units. Cost of piping was also higher for SCEPPHAR because of its more complex liquid interchange system.

Operational expenditures (OPEX) were slightly higher for SCEPPHAR, mainly due to the higher maintenance costs related to the higher CAPEX. The wastewater tariff required to obtain an IRR = 4% was 0.27 and 0.31 €/m^3 for A^2/O and SCEPPHAR, respectively. Hence, SCEPPHAR is outcompeted by a conventional A^2/O if only the incomes from biogas production and struvite are considered. However, the difference in terms of wastewater tariff aid for SCEPPHAR is only 15% higher than for A^2/O.

4. Discussion

4.1. COD requirements for the SCEPPHAR configuration

The pilot plant during Period III showed good removal efficiencies of P (94 ± 12%) and N (82 ± 11) with a wastewater enriched in VFA: $COD_T = 338 \pm 81\ mgCOD\cdot L^{-1}$, $COD_S = 236 \pm 39\ mgCOD\cdot L^{-1}$, ammonium 40 ± 11 mg $NH_4^+\text{-}N\cdot L^{-1}$ and phosphate 4.2 ± 1.1 mg $PO_4^{3-}\text{-}P\cdot L^{-1}$. Metcalf and Eddy (Tchobanoglous et al., 2013) recommend threshold ratios for the design of WWTP configurations aiming at simultaneous C, N and P removal (A^2/O and UCT): a readily biodegradable COD (rbCOD) content of 6.6 g $rbCOD\cdot g^{-1}NO_3^-\text{-}N$ and 10 g $rbCOD\cdot g^{-1}P$. These ratios, translated to the wastewater treated in this work, result in the need of 306 g $rbCOD\cdot L^{-1}$. This value is higher than the CODs available for the VFA-enriched wastewater treated in this work (236 ± 39 $mgCOD\cdot L^{-1}$). Hence, if the wastewater met the design recommendation of Metcalf and Eddy, the SCEPPHAR configuration would be able to treat it without the need of adding extra COD.

If the COD concentration was too low, as in the case studied in this work, additional VFA would be required. Fermentation of excess sludge appears as a clear option to obtain extra VFA, although the amount produced is highly dependent on the

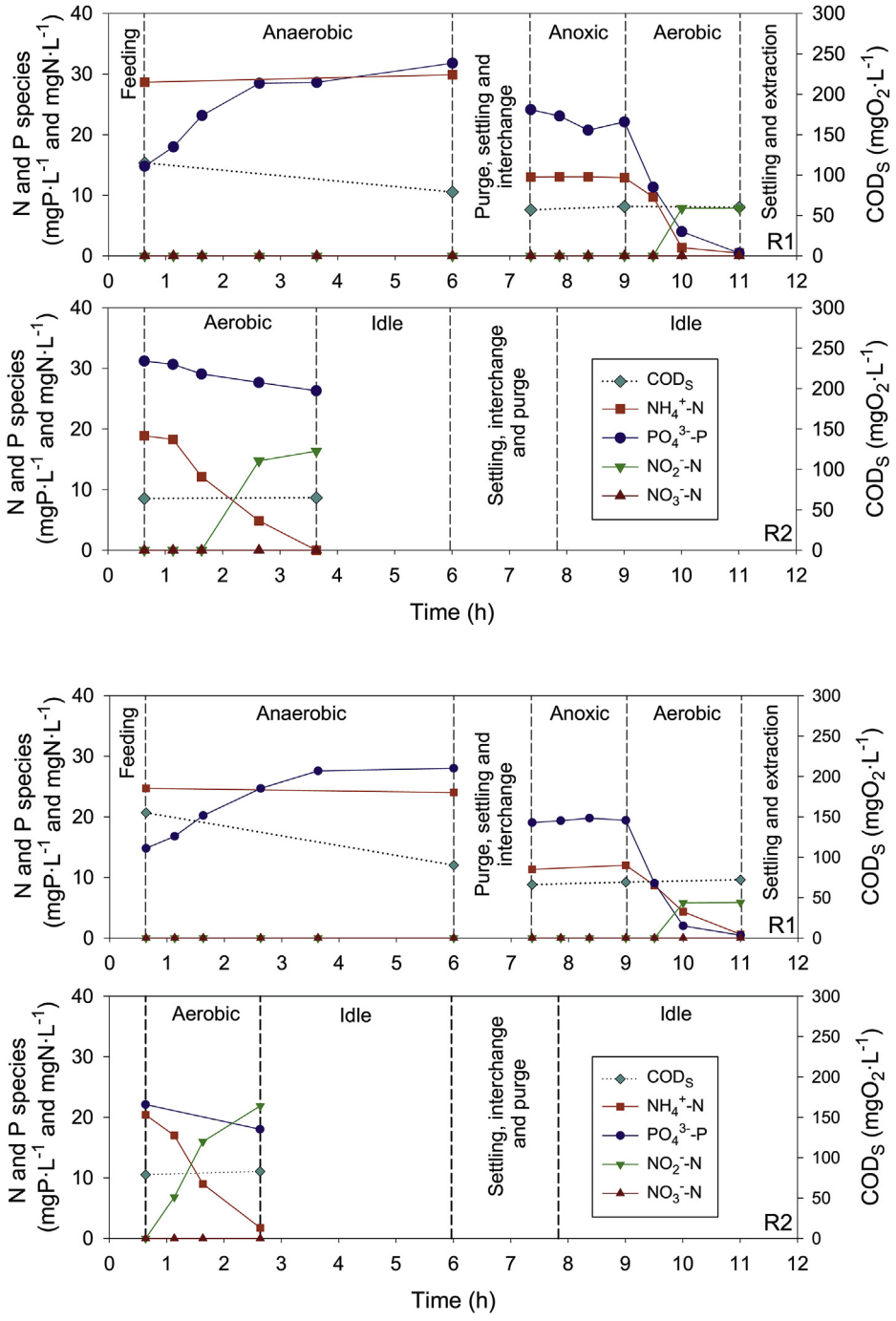

Fig. 6. Period III. Example of two SCEPPHAR pilot-plant cycles (days 410 and 439) with N-removal via nitrite.

pretreatments used (Longo et al., 2015; Luo et al., 2019). For the R1-HET scenario (i.e. SRT around 10 d and with 2.7 $gTSS \cdot L^{-1}$) the solids production would be around 675 $gTSS \cdot d^{-1}$. To obtain an increase of VFA in the influent around 100 $mgCOD \cdot L^{-1}$ for a daily influent of 3500 L d^{-1}, 350 $gCOD \cdot d^{-1}$ would be required. Considering a ratio of 0.85 $gTVS \cdot g^{-1}TSS$ in the sludge, this amount of COD could be obtained achieving a fermentation yield of 0.61 $gCOD \cdot g^{-1}TVS$ by using one of the pretreatments reported in the literature (Luo et al., 2019). Additional COD could be also obtained from the fermentation of primary sludge or other fermentable carbon sources such as glycerol (Guerrero et al., 2015, 2012).

4.2. Successful implementation of nitrite shortcut

The simultaneous implementation of real-time control of the length of the aerobic phase and decrease of SRT led to a successful operation with shortcut N-removal, that was maintained without observing any NOB adaptation during the operation of Period III. The rationale of the first strategy is that if aeration is switched off around complete ammonia oxidation, some residual nitrite should be present that could not be further oxidised by NOB due to the lack of aeration, thereby limiting their growth (Fux et al., 2006; Guisasola et al., 2010; Guo et al., 2009; Lemaire et al., 2008;

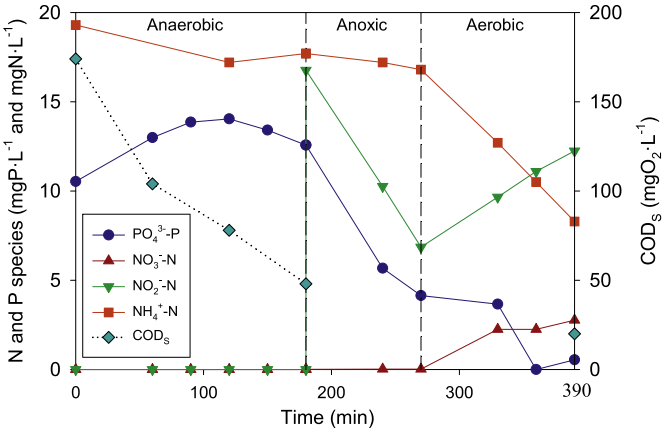

Fig. 7. Batch experiment with nitrite as electron acceptor under anoxic conditions, performed on day 419 of operation with biomass obtained from R1-HET.

Marcelino et al., 2011). The reduced NOB growth would lead to a slightly lower nitrite oxidation rate in the following cycle. As a result, nitrite accumulation when ammonia oxidation is completed and the aeration phase is terminated would be slightly higher than in the previous cycle, further reducing the growth of NOB. Over many cycles, the NOB population would decrease gradually, which will be accompanied by increased nitrite accumulation at the end of the aeration phases. While NOB growth is repressed through this misalignment between oxygen and nitrite, AOB are not affected because oxygen is provided until ammonium is depleted. Moreover, it may also result in transitory high free nitrous acid (FNA) levels when aeration is terminated and nitrite is accumulated in the bulk liquid. While the reported FNA levels inhibitory to AOB and NOB varied considerably in different studies, it is evident that AOB are in general much more tolerant to FNA than NOB (Jubany et al., 2009b; Park and Bae, 2009). In summary, when aeration is suppressed, the conditions are set so that it is likely that μ_{NOB} decreases more than μ_{AOB}, thus contributing to the decrease of NOB activity. This strategy can only be successful if it is combined with a proper SRT selected to remove NOB faster than they grow as shown in equation (1) and explained in previous works (Guisasola et al., 2010; Jubany et al., 2009a, 2009b; Lemaire et al., 2008; Marcelino et al., 2011).

4.3. Resource recovery

Most alternatives to recover P from WRRFs are based on the sludge generated (Cieślik and Konieczka, 2017; Egle et al., 2016; Mayer et al., 2016; Melia et al., 2017; Rittmann et al., 2011; Rotta et al., 2019). The most accepted strategy is, nowadays, its precipitation as struvite ($NH_4MgPO_4 \cdot 6H_2O$) from the supernatant of digested sludge (Jabr et al., 2019; Le Corre et al., 2009; Li et al., 2019; Rittmann et al., 2011). Struvite is a slow-release rate fertiliser with nitrogen and magnesium that has been reported to be a good option for agricultural uses. Struvite precipitation in a tertiary step is not a viable option due to the low concentration of phosphate and ammonia. The most adequate stream for the struvite precipitation is the digestate of anaerobic digestion, due to its high ammonia and phosphate concentrations. In addition, when EBPR is integrated in a WRRF, P recovery as struvite from the digestate can be more efficient since the sludge entering anaerobic digestion contains up to 20 times more P as Poly-P that could be easily released in the digestate (Münch and Barr, 2001; Shu et al., 2006).

However, typical values of P-recovery around 12% are obtained by struvite precipitation from the supernatant of anaerobic digestion (Remy and Jossa, 2015), in contrast to the much higher 45–63% of P-recovery reported in section 3.4, which is one of the main achievements of the mainstream SCEPPHAR.

The key operational factor in this configuration is obtaining a high anaerobic P-release, as it determines the maximum resource recovery that can be obtained: the amount of P that can be recovered in R3-PRE and the percentage of PHA in the sludge. On the other hand, the precipitation reactor does not need to be designed to treat all the influent wastewater, as less than 9% of the influent is treated in this case (5.5% of the reactor volume). Another possibility would be decreasing the number of cycles with precipitation: it could be plan a single recovery per day with some extra VFA in this specific cycle. This strategy has been proposed in the literature (Kodera et al., 2013; Lv et al., 2014), although in some cases it has provoked some instability in PAO activity (Acevedo et al., 2015). Nevertheless, the long-term operation with an optimised volume of anaerobic supernatant extraction every cycle has been demonstrated to be feasible and stable at lab-scale (Guisasola et al., 2019).

With respect to PHA, the values of 6.9% at the end of the anaerobic phase or 9.1% after adding extra VFA obtained in this work are much lower than the 41% ($gPHA \cdot g^{-1}VSS$) obtained by a

Table 5
P release and COD consumption rates during R1-HET anaerobic phase.

Cycle	P-release	P-release rate	COD consumption rate	P/C ratio
	$mgP \cdot L^{-1}$	$mgP \cdot mg^{-1}VSS \cdot min^{-1}$	$mgCOD \cdot mg^{-1}VSS \cdot min^{-1}$	molP/molC
Day 139	31.0	0.129	0.212	0.35
Day 362	12.0	0.044	na	na
Day 410	27.0	0.096	0.055	0.68
Day 439	23.2	0.051	0.094	0.32

na: not available.

Table 6
Ammonium consumption and nitrite and nitrate production rates in R2-AUT for the four cycles presented.

Test	NH_4^+-N oxid.	NO_2^--N prod.	NO_3^--N prod.	NO_3^--N/NH_4^+-N	NO_2^--N/NH_4^+-N
	$gN \cdot g^{-1}VSS \cdot min^{-1}$	$gN \cdot g^{-1}VSS \cdot min^{-1}$	$gN \cdot g^{-1}VSS \cdot min^{-1}$	–	
Day 139	0.035	0.000	0.047	1.36	0.00
Day 362	0.029	0.000	0.027	0.94	0.00
Day 410	0.062	0.062	0.000	0.00	1.01
Day 439	0.087	0.122	0.000	0.00	1.40

side-stream system fed with surplus full-scale activated sludge and acclimated with fest/famine cycles using fermented VFA liquors from industry or primary sludge sources (Werker et al., 2018). However, considering the amount of sludge produced per day and the COD load in the pilot plant, our 6.9% of PHA in the biomass results in a yield around 5% of the inlet COD finally ending as PHA in the produced sludge. This result seems low at a first glance, but it is much higher than the negligible yields that can be obtained in side-stream systems for producing PHA.

The PHA content in the biomass could be even improved if R1-HET was operated at a lower SRT. This lower SRT would decrease the total biomass and, thus, would increase the percentage of PHA in the sludge if enough anaerobic VFA uptake is maintained. In a previous work (Chan et al., 2020), the PHA content of EBPR biomass increased from 8 to 18% ($gPHA \cdot g^{-1}VSS$) when the SRT was decreased from 15 to 5 days. This change can easily be implemented in the mainstream SCEPPHAR configuration, since it is a two-sludge system that allows the independent optimization of both SRT.

To elucidate if the experimental PHA content in the biomass was reasonable, the amount of PHA produced with the extra VFA added was calculated considering the anaerobic stoichiometry for PAO (Smolders et al., 1994) (1.33 $molC\text{-}PHB \cdot mol^{-1}C\text{-}Acet$ = 0.95 $gPHB \cdot g^{-1}Acet$). The inlet acetic acid (100 $mgCOD \cdot L^{-1}$) to R1-HET with a typical biomass concentration of 2.7 $gTSS \cdot L^{-1}$ would result in an increase of 2.5% of the PHA percentage in the biomass. Therefore, the experimental PHA increase observed (3.8%) was reasonable, as some of the inlet COD could be fermented to VFA during the anaerobic phase. In the hypothetic case that the biomass concentration was only 1.4 $gTSS \cdot L^{-1}$, the increase of PHA would have been 4.8%, which supports the strategy of decreasing SRT for increasing the percentage of PHA. These results also show that an important amount of VFA should be available or added in view of obtaining biomass with a significant PHA percentage.

Although the experimental PHA content obtained could be improved by lowering SRT or with sporadic VFA dosages, its percentage is still far from the requirements for an economical downstream recovery of the PHA polymer, which recommends a minimum value of 40% ($gPHA \cdot g^{-1}VSS$) (Werker et al., 2018). Nevertheless, purging sludge with high PHA content can also be beneficial for an enhanced biogas production. Several works report a significant increase of biomethane potential (BMP) of biomass with higher PHA content (Guisasola et al., 2019; Huda et al., 2016; Wang et al., 2016). Chan et al. (2020) studied BMP versus the PHA content in EBPR sludge at different operational conditions and obtained a linear correlation BMP ($mL\ CH4 \cdot g^{-1}VSS$) = 240 + 15.3 * PHA ($mmol\ C \cdot g^{-1}VSS$). They showed that the percentage of COD in the influent that could be recovered as methane could be increased from 11% (SRT = 15 d and purge extracted from the aerobic reactor) to 28% (SRT = 5 d and purge extracted from the anaerobic reactor). Moreover, the main BMP increase was observed during the first days of the test, due to the higher biodegradability of PHA. Thus, digesting biomass with high PHA content would have a significant impact in anaerobic digesters working at relatively low HRT.

4.4. Integrated assessment

This work reports the major benefits of the mainstream SCEPPHAR configuration: i) EBPR can be combined with a high P recovery as struvite, ii) the sludge generated contains a higher amount of PHA than conventional sludge, iii) it can remove nitrogen via nitrite shortcut, and iv) high COD, N and P removal are stably obtained if enough rbCOD is available in the wastewater. On the other hand, the PHA content in the sludge does not allow an economically feasible extraction, although this sludge increases the specific biogas production. Struvite recovery is demonstrated, but the incomes that could be obtained are nowadays negligible compared to the other costs. Current CAPEX estimation for the SCEPPHAR configuration is higher than for a typical A^2/O configuration without resource recovery, and hence, further development and optimization is needed to become competitive from an economic point of view. The 15% higher wastewater tariff required for SCEPPHAR than for A^2/O could justify its implementation if resource recovery is considered strategic and incentives are legislated. The current study did not consider incomes from PHA because of its concentration below the recommended 40%. However, evidences from other projects, e.g. PHARIO (Bengsston et al., 2017; Werker et al., 2018), suggest that a PHA accumulation up to 40% is feasible if short enrichment periods are planned at the expense of an additional reactor and external VFA dosage. This would open the possibility to obtain incomes from PHA recovery in SCEPPHAR that would potentially improve its economic feasibility (Bengsston et al., 2017).

5. Conclusions

The mainstream SCEPPHAR configuration was operated in a demo-scale pilot plant and for a long-term with successful results in terms of C, N and P removal efficiencies under full nitrification and under nitrite shortcut mode.

- Regarding P recovery, the anaerobic supernatant had a concentration of P of 6–9 times that of the influent, allowing that 45–63% of the P in the influent could be recovered as struvite in a separate precipitator. This value is much higher than the typical values around 12% reported for sidestream P-recovery.
- Mainstream SCEPPHAR proposes a purge from the anaerobic phase of the EBPR system rather the conventional purging at the end of the aerobic phase. This biomass contains 6.9–9.2% of PHA, a higher percentage than typical activated sludge, but its extraction does not seem economically feasible for bioplastic production with the current technologies. Nevertheless, purging biomass with high PHA content would increase the methane production when diverting this sludge to anaerobic digestion and, thus, it would enhance the energy recovery of the system.
- The economic feasibility study shows that the current SCEPPHAR technology would require a water tariff 15% higher than that of a conventional A^2/O and hence it would be necessary to legislate incentives to favour resource recovery to make it economically viable.

Declaration of competing interest

The authors declare that they have no known competing financial interests or personal relationships that could have appeared to influence the work reported in this paper.

Acknowledgements

This work was funded by the SMART-Plant project (Scale-up of low-carbon footprint Material Recovery Techniques, EUH2020, grant agreement 690323). Oriol Larriba is grateful to the FI predoctoral scholarship from the Catalan Government (2019FI-B1-00051). The authors are members of the GENOCOV research group (Grup de Recerca Consolidat de la Generalitat de Catalunya, 2017 SGR 1175, www.genocov.com). The authors want to acknowledge the support on field by Anna Lupón, David Güell and Ricard Tomás from Aigües de Manresa. Special thanks to Borja Solís for his support during the plant operation.

Appendix A. Supplementary data

Supplementary data to this article can be found online at https://doi.org/10.1016/j.watres.2020.115474.

References

Acevedo, B., Camiña, C., Corona, J.E., Borrás, L., Barat, R., 2015. The metabolic versatility of PAOs as an opportunity to obtain a highly P-enriched stream for further P-recovery. Chem. Eng. J. 270, 459–467. https://doi.org/10.1016/j.cej.2015.02.063.

Ahmed, M., Hasan, C.K., Rahman, H., Ali Hossain, M., Uddin, S.A., 2015. Prospects of using wastewater as a resource-nutrient recovery and energy generation. Am. J. Environ. Sci. 11, 99–114. https://doi.org/10.3844/ajessp.2015.98.114.

APHA, 1995. Standard Methods for the Examination of Water and Wastewater. American Public Health Association, Washington, DC. USA.

Aslan, S., Miller, L., Dahab, M., 2009. Ammonium oxidation via nitrite accumulation under limited oxygen concentration in sequencing batch reactors. Bioresour. Technol. 100, 659–664. https://doi.org/10.1016/j.biortech.2008.07.033.

Baeza, J.A., Guerrero, J., Guisasola, A., 2017. Optimising a novel SBR configuration for enhanced biological phosphorus removal and recovery (EBPR^2). Desalin. Water Treat. 68 https://doi.org/10.5004/dwt.2017.20468.

Bengsston, S., Werker, A., Visser, C., Korving, L., 2017. PHARIO Stepping stone to a sustainable vaue chain for PHA bioplastic using municipal activated sludge. STOWA Report 2017-15.

Blackburne, R., Yuan, Z., Keller, J., 2008. Partial nitrification to nitrite using low dissolved oxygen concentration as the main selection factor. Biodegradation 19, 303–312. https://doi.org/10.1007/s10532-007-9136-4.

Chan, C., Guisasola, A., Baeza, J.A., 2020. Correlating the biochemical methane potential of bio-P sludge with its polyhydroxyalkanoate content. J. Clean. Prod. 242 https://doi.org/10.1016/j.jclepro.2019.118495, 118495.

Cieślik, B., Konieczka, P., 2017. A review of phosphorus recovery methods at various steps of wastewater treatment and sewage sludge management. The concept of “no solid waste generation” and analytical methods. J. Clean. Prod. 142, 1728–1740. https://doi.org/10.1016/j.jclepro.2016.11.116.

Cordell, D., Rosemarin, A., Schröder, J.J., Smit, A.L., 2011. Towards global phosphorus security: a systems framework for phosphorus recovery and reuse options. Chemosphere 84, 747–758. https://doi.org/10.1016/j.chemosphere.2011.02.032.

EEC Council, 1991. Council Directive of 21 May 1991 concerning urban waste water treatment (91/271/EEC). Off. J. Eur. Communities.

Egle, L., Rechberger, H., Krampe, J., Zessner, M., 2016. Phosphorus recovery from municipal wastewater: an integrated comparative technological, environmental and economic assessment of P recovery technologies. Sci. Total Environ. 571, 522–542. https://doi.org/10.1016/j.scitotenv.2016.07.019.

Fux, C., Velten, S., Carozzi, V., Solley, D., Keller, J., 2006. Efficient and stable nitritation and denitritation of ammonium-rich sludge dewatering liquor using an SBR with continuous loading. Water Res. 40, 2765–2775. https://doi.org/10.1016/j.watres.2006.05.003.

Guerrero, J., Guisasola, A., Baeza, J.A., 2015. Controlled crude glycerol dosage to prevent EBPR failures in C/N/P removal WWTPS. Chem. Eng. J. 271, 114–127. https://doi.org/10.1016/j.cej.2015.02.062.

Guerrero, J., Tayà, C., Guisasola, A., Baeza, J.A., 2012. Glycerol as a sole carbon source for enhanced biological phosphorus removal. Water Res. 46, 2983–2991. https://doi.org/10.1016/j.watres.2012.02.043.

Guisasola, A., Chan, C., Larriba, O., Lippo, D., Suárez-Ojeda, M.E., Baeza, J.A., 2019. Long-term stability of an enhanced biological phosphorus removal system in a phosphorus recovery scenario. J. Clean. Prod. 214, 308–318. https://doi.org/10.1016/j.jclepro.2018.12.220.

Guisasola, A., Marcelino, M., Lemaire, R., Baeza, J.A., Yuan, Z., 2010. Modelling and simulation revealing mechanisms likely responsible for achieving the nitrite pathway through aeration control. Water Sci. Technol. 61, 1459. https://doi.org/10.2166/wst.2010.017.

Guisasola, A., Vargas, M.D.M., Marcelino, M., Lafuente, F.J., Casas, C., Baeza, J.A., 2007. On-line monitoring of the enhanced biological phosphorus removal process using respirometry and titrimetry. Biochem. Eng. J. 35, 371–379. https://doi.org/10.1016/j.bej.2007.02.001.

Guo, J.H., Peng, Y.Z., Wang, S.Y., Zheng, Y.N., Huang, H.J., Ge, S.J., 2009. Effective and robust partial nitrification to nitrite by real-time aeration duration control in an SBR treating domestic wastewater. Process Biochem. 44, 979–985. https://doi.org/10.1016/j.procbio.2009.04.022.

Huda, S.M.S., Satoh, H., Mino, T., 2016. Anaerobic degradation of polyhydroxyalkanoate accumulated in activated sludge in the absence of anaerobic digested sludge. J. Water Environ. Technol. 14, 236–246. https://doi.org/10.2965/jwet.15-037.

Jabr, G., Saidan, M., Al-Hmoud, N., 2019. Phosphorus recovery by struvite formation from Al Samra municipal wastewater treatment plant in Jordan. Desalin. Water Treat. 146, 315–325. https://doi.org/10.5004/dwt.2019.23608.

Jiang, C., Xu, S., Wang, R., Feng, S., Zhou, S., Wu, Shimin, Zeng, X., Wu, Shanghua, Bai, Z., Zhuang, G., Zhuang, X., 2019. Achieving efficient nitrogen removal from real sewage via nitrite pathway in a continuous nitrogen removal process by combining free nitrous acid sludge treatment and DO control. Water Res. 161, 590–600. https://doi.org/10.1016/J.WATRES.2019.06.040.

Jianlong, W., Ning, Y., 2004. Partial nitrification under limited dissolved oxygen conditions. Process Biochem. 39, 1223–1229. https://doi.org/10.1016/S0032-9592(03)00249-8.

Jubany, I., Baeza, J.A., Lafuente, F.J., Carrera, J., 2009a. Model-based study of nitrite accumulation with OUR control in two continuous nitrifying activated sludge configurations. Water Sci. Technol. 60, 2685–2693. https://doi.org/10.2166/wst.2009.694.

Jubany, I., Lafuente, F.J., Baeza, J.A., Carrera, J., 2009b. Total and stable washout of nitrite oxidizing bacteria from a nitrifying continuous activated sludge system using automatic control based on Oxygen Uptake Rate measurements. Water Res. 43, 2761–2772. https://doi.org/10.1016/j.watres.2009.03.022.

Kodera, H., Hatamoto, M., Abe, K., Kindaichi, T., Ozaki, N., Ohashi, A., 2013. Phosphate recovery as concentrated solution from treated wastewater by a PAO-enriched biofilm reactor. Water Res. 47, 2025–2032. https://doi.org/10.1016/j.watres.2013.01.027.

Le Corre, K.S., Valsami-Jones, E., Hobbs, P., Parsons, S.A., 2009. Phosphorus recovery from wastewater by struvite crystallization: a review. Crit. Rev. Environ. Sci. Technol. 39, 433–477.

Lemaire, R., Marcelino, M., Yuan, Z., 2008. Achieving the nitrite pathway using aeration phase length control and step-feed in an SBR removing nutrients from abattoir wastewater. Biotechnol. Bioeng. 100, 1228–1236. https://doi.org/10.1002/bit.21844.

Li, B., Boiarkina, I., Yu, W., Huang, H.M., Munir, T., Wang, G.Q., Young, B.R., 2019. Phosphorous recovery through struvite crystallization: challenges for future design. Sci. Total Environ. 648, 1244–1256. https://doi.org/10.1016/j.scitotenv.2018.07.166.

Lizarralde, I., Fernández-Arévalo, T., Manas, A., Ayesa, E., Grau, P., 2019. Model-based opti mization of phosphorus management strategies in Sur WWTP. Madrid. Water Res 153, 39–52. https://doi.org/10.1016/j.watres.2018.12.056.

Longo, S., Katsou, E., Malamis, S., Frison, N., Renzi, D., Fatone, F., 2015. Recovery of volatile fatty acids from fermentation of sewage sludge in municipal wastewater treatment plants. Bioresour. Technol. 175, 436–444. https://doi.org/10.1016/j.biortech.2014.09.107.

Luo, K., Pang, Y., Yang, Q., Wang, D., Li, X., Lei, M., Huang, Q., 2019. A critical review of volatile fatty acids produced from waste activated sludge: enhanced strategies and its applications. Environ. Sci. Pollut. Res. 26, 13984–13998. https://doi.org/10.1007/s11356-019-04798-8.

Lv, J.-H., Yuan, L.-J., Chen, X., Liu, L., Luo, D.-C., 2014. Phosphorus metabolism and population dynamics in a biological phosphate-removal system with simultaneous anaerobic phosphate stripping. Chemosphere 117C, 715–721. https://doi.org/10.1016/j.chemosphere.2014.10.018.

Ma, Y., Peng, Y., Wang, S., Yuan, Z., Wang, X., 2009. Achieving nitrogen removal via nitrite in a pilot-scale continuous pre-denitrification plant. Water Res. 43, 563–572. https://doi.org/10.1016/j.watres.2008.08.025.

Marcelino, M., Wallaert, D., Guisasola, A., Baeza, J.A., 2011. A two-sludge system for simultaneous biological C, N and P removal via the nitrite pathway. Water Sci. Technol. 64, 1142–1147. https://doi.org/10.2166/wst.2011.398.

Massara, T.M., Malamis, S., Guisasola, A., Baeza, J.A., Noutsopoulos, C., Katsou, E., 2017. A review on nitrous oxide (N2O) emissions during biological nutrient removal from municipal wastewater and sludge reject water. Sci. Total Environ. 596–597. https://doi.org/10.1016/j.scitotenv.2017.03.191.

Massara, T.M., Solís, B., Guisasola, A., Katsou, E., Baeza, J.A., 2018. Development of an ASM2d-N2O model to describe nitrous oxide emissions in municipal WWTPs under dynamic conditions. Chem. Eng. J. 335, 185–196. https://doi.org/10.1016/j.cej.2017.10.119.

Mayer, B.K., Baker, L.A., Boyer, T.H., Drechsel, P., Gifford, M., Hanjra, M.A., Parameswaran, P., Stoltzfus, J., Westerhoff, P., Rittmann, B.E., 2016. Total value of phosphorus recovery. Environ. Sci. Technol. 50 https://doi.org/10.1021/acs.est.6b01239.

Meijer, S.C., van Loosdrecht, M.C.M., Heijnen, J.J., 2001. Metabolic modelling of full-scale biological nitrogen and phosphorus removing wwtp's. Water Res. 35, 2711–2723.

Melia, P.M., Cundy, A.B., Sohi, S.P., Hooda, P.S., Busquets, R., 2017. Trends in the recovery of phosphorus in bioavailable forms from wastewater. Chemosphere 186, 381–395. https://doi.org/10.1016/j.chemosphere.2017.07.089.

Montiel-Jarillo, G., Carrera, J., Suárez-Ojeda, M.E., 2017. Enrichment of a mixed microbial culture for polyhydroxyalkanoates production: effect of pH and N and P concentrations. Sci. Total Environ. 583, 300–307. https://doi.org/10.1016/j.scitotenv.2017.01.069.

Münch, E.V., Barr, K., 2001. Controlled struvite crystallisation for removing phosphorus from anaerobic digester sidestreams. Water Res. 35, 151–159. https://doi.org/10.1016/S0043-1354(00)00236-0.

Park, S., Bae, W., 2009. Modeling kinetics of ammonium oxidation and nitrite oxidation under simultaneous inhibition by free ammonia and free nitrous acid. Process Biochem. 44, 631–640. https://doi.org/10.1016/j.procbio.2009.02.002.

Pollice, A., Tandoi, V., Lestingi, C., 2002. Influence of aeration and sludge retention time on ammonium oxidation to nitrite and nitrate. Water Res. 36, 2541–2546.

Remy, C., Jossa, P., 2015. Life Cycle Assessment of Selected Processes for P Recovery from Sewage Sludge, Sludge Liquor, or Ash. Deliverable 9.2 of P-REX Project. Sustainable Sewage Sludge Management Fostering Phosphorus Recovery and Energy Efficiency.

Rey-Martínez, N., Badia-Fabregat, M., Guisasola, A., Baeza, J.A., 2019. Glutamate as sole carbon source for enhanced biological phosphorus removal. Sci. Total Environ. 657, 1398–1408. https://doi.org/10.1016/j.scitotenv.2018.12.064.

Rittmann, B.E., Mayer, B., Westerhoff, P., Edwards, M., 2011. Capturing the lost phosphorus. Chemosphere 84, 846–853. https://doi.org/10.1016/

j.chemosphere.2011.02.001.
Rotta, E.H., Bitencourt, C.S., Marder, L., Bernardes, A.M., 2019. Phosphorus recovery from low phosphate-containing solution by electrodialysis. J. Membr. Sci. 573, 293–300. https://doi.org/10.1016/j.memsci.2018.12.020.
Shi, J., Lu, X., Yu, R., Zhu, W., 2012. Nutrient removal and phosphorus recovery performances of a novel anaerobic-anoxic/nitrifying/induced crystallization process. Bioresour. Technol. 121, 183–189. https://doi.org/10.1016/j.biortech.2012.06.064.
Shu, L., Schneider, P., Jegatheesan, V., Johnson, J., 2006. An economic evaluation of phosphorus recovery as struvite from digester supernatant. Bioresour. Technol. 97, 2211–2216. https://doi.org/10.1016/j.biortech.2005.11.005.
Smolders, G.J.F., van der Meij, J., van Loosdrecht, M.C.M., Heijnen, J.J., 1994. Model of the anaerobic metabolism of the biological phosphorus removal process: stoichiometry and pH influence. Biotechnol. Bioeng. 43, 461–470. https://doi.org/10.1002/bit.260430605.
Tayà, C., Garlapati, V.K., Guisasola, A., Baeza, J.A., 2013. The selective role of nitrite in the PAO/GAO competition. Chemosphere 93, 612–618. https://doi.org/10.1016/j.chemosphere.2013.06.006.
Tchobanoglous, G., Burton, F.L., Stensel, H.D., 2013. Wastewater Engineering: Treatment and Reuse, Fourth. ed. Metcalf & Eddy, Inc., New York. McGraw-Hill.
Theregowda, R.B., González-Mejía, A.M., Ma, X., (Cissy), Garland, J., 2019. Nutrient recovery from municipal wastewater for sustainable food production systems: an alternative to traditional fertilizers. Environ. Eng. Sci. 36, 833–842. https://doi.org/10.1089/ees.2019.0053.
Türk, O., Mavinic, D.S., 1987. Benefits of using selective inhibition to remove nitrogen from highly nitrogenous wastes. Environ. Technol. Lett 8, 419–426. https://doi.org/10.1080/09593338709384500.
Valverde-Pérez, B., Ramin, E., Smets, B.F., Plósz, B.G., 2015. EBP2R – an innovative enhanced biological nutrient recovery activated sludge system to produce growth medium for green microalgae cultivation. Water Res. 68, 821–830. https://doi.org/10.1016/j.watres.2014.09.027.
van Loosdrecht, M.C.M., Brandse, F., De Vries, A., 1998. Upgrading of waste water treatment processes for integrated nutrient removal-the BCFS® process. Water Sci. Technol. 37, 209–217.
Wang, D.-B., Li, X.-M., Yang, Q., Zheng, W., Wu, Y., Zeng, T., Zeng, G., 2012. Improved Biological Phosphorus Removal Performance Driven by the Aerobic/extended-Idle Regime with Propionate as the Sole Carbon Source, Water Research. https://doi.org/10.1016/j.watres.2012.04.036.
Wang, Q., Sun, J., Zhang, C., Xie, G.-J., Zhou, X., Qian, J., Yang, G., Zeng, G., Liu, Y., Wang, D., 2016. Polyhydroxyalkanoates in waste activated sludge enhances anaerobic methane production through improving biochemical methane potential instead of hydrolysis rate. Sci. Rep. 6, 19713. https://doi.org/10.1038/srep19713.
Werker, A., Bengtsson, S., Korving, L., Hjort, M., Anterrieu, S., Alexandersson, T., Johansson, P., Karlsson, A., Karabegovic, L., Magnusson, P., Morgan-Sagastume, F., Sijstermans, L., Tietema, M., Visser, C., Wypkema, E., van der Kooij, Y., Deeke, A., Uijterlinde, C., 2018. Consistent production of high quality PHA using activated sludge harvested from full scale municipal wastewater treatment – PHARIO. Water Sci. Technol. 78, 2256–2269. https://doi.org/10.2166/wst.2018.502.
Werker, A., Lind, P., Bengtsson, S., Nordström, F., 2008. Chlorinated-solvent-free gas chromatographic analysis of biomass containing polyhydroxyalkanoates. Water Res. 42, 2517–2526. https://doi.org/10.1016/j.watres.2008.02.011.
Yang, Q., Peng, Y., Liu, X., Zeng, W., Mino, T., Satoh, H., 2007. Nitrogen removal via nitrite from municipal wastewater at low temperatures using real-time control to optimize nitrifying communities. Environ. Sci. Technol. 41, 8159–8164. https://doi.org/10.1021/es070850f.